

We are IntechOpen, the world's leading publisher of Open Access books Built by scientists, for scientists

6,900

Open access books available

185,000

International authors and editors

200M

Downloads

Our authors are among the

154

Countries delivered to

TOP 1%

most cited scientists

12.2%

Contributors from top 500 universities



WEB OF SCIENCE™

Selection of our books indexed in the Book Citation Index
in Web of Science™ Core Collection (BKCI)

Interested in publishing with us?
Contact book.department@intechopen.com

Numbers displayed above are based on latest data collected.
For more information visit www.intechopen.com



DBDP SAR Microstrip Array Technology

Shun-Shi Zhong

*School of Communication and Information Engineering
Shanghai University, Shanghai 200072
China*

1. Introduction

1.1 Background

Since the American satellite SEASAT was launched in June 1978, an era for the space-borne synthetic aperture radar (SAR) systems has been started. Over 30 years from then on, more and more SAR systems have been proposed and manufactured, such as: ALMAZ SAR system ejected by the former U.S.S.R in 1991, ERS-1 of European Space Agency (ESA) in 1991, JERS-1 of Japan in 1992, RadarSat-1 and RadarSat-2 of Canada in 1995 and 2005, Terra SAR-X of German in 2007 and RiSat-SAR of India in 2007, etc. Another milestone is that the SIR- C/X SAR of American Space Shuttle Endeavour completed the high resolution three-dimensional (3D) imaging all over the globe in Feb. 2000.

The overall performances of a SAR system such as azimuth/elevation resolution, imaging ambiguity, width of mapping area and so on are directly determined by the performance of its antenna. Since the response of an object to the electromagnetic wave with different polarization is different, the dual-polarization operation of the antenna can provide additional information and thus the probability of detecting and identifying a target is enhanced. Because that the reflection characteristic of an object is various for the incident electromagnetic wave with different frequency, its multi-band operation will provide more information such as the back-scattering data and the penetration data of objects. The common bands of space-borne SARs are L (center at 1.275 GHz), S (3.0 GHz), C (5.3 GHz) and X (9.6 GHz) bands. For example, the SIR-C/X-SAR system uses L/C/X tri-bands with dual-polarization, whose advantages were proved and the function of 3D mapping was realized by the use of interference imaging [1]. However, as seen from Fig. 1, its antenna consists of three sub-arrays separately for L, C, X bands with $12\text{ m} \times 4.1\text{ m}$ area, resulting in a bulky structure of about 3000 kg weight. The realization of a shared-aperture configuration will minimize the volume and weight of the antenna and share the sub-systems behind the array as well. Therefore, the dual-band dual-polarization (DBDP) shared-aperture antenna array has been proposed and studied. In China, following many researches on the dual-polarized planar antenna arrays [2–6], the development of DBDP arrays has also been carried out [7–9].

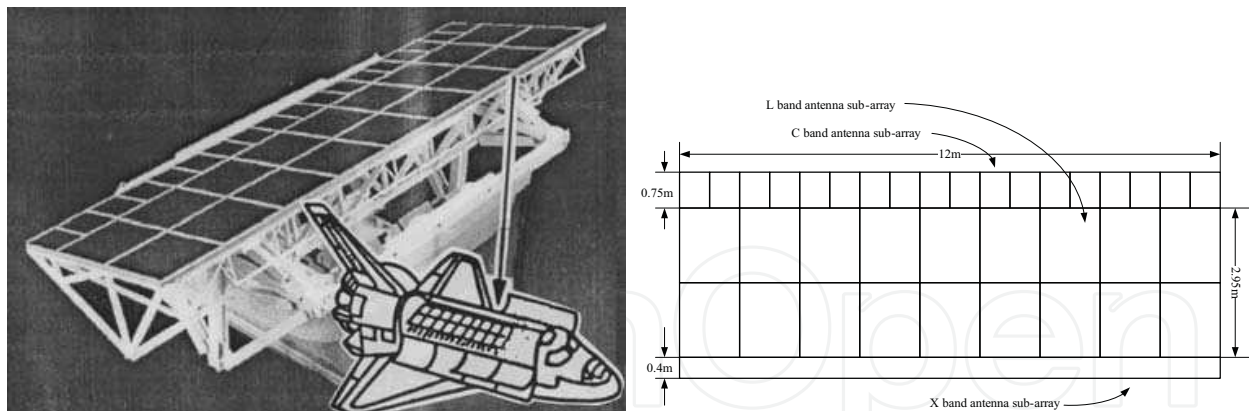


Fig. 1. Antenna of SIR-C/X SAR

1.2 Design principles

The dual-band and dual-polarized operation of an antenna has been applied in a lot of systems, such as wireless communications, radars, deep space communications and radio astronomical telescopes, etc. The requirements for antennas are varied in different missions, and thus the designs are different, especially for the latter two where the reflector antennas are preferred while a horn or a small patch array may be used as the feed [10, 11].

This paper emphasizes the DBDP antennas for SAR application. For the future remote sensing mission, two-plane phased scanning characteristics are needed, so generally the possibility of using reflector antennas is excluded. Meanwhile, although the waveguide slotted antenna array has better efficiency and sidelobe characteristics, it is still not preferred in future SAR application, because it is hard to realize two-plane phased scanning/ beam-forming DBDP operation and its mass is large [6], then the microstrip patch array becomes the best choice. Due to that the operation frequencies of different bands in the DBDP SAR application are widely separated, it is difficult to use dual-frequency radiator element to construct a DBDP antenna array. Thus it comes as an obvious alternative to construct a DBDP antenna by integrating the radiators for each individual band. And apparently, the multi-layer configuration is required to contain two individual band elements and their feed networks. In addition, the cross-polarization of the array should be less than -30 dB or it will cause imaging ambiguity, and the isolation between dual polarization ports should also be considered carefully. Since the bandwidth impacts the elevation resolution directly, a wide bandwidth is more an important target.

According to the configuration, the typical DBDP arrays include: the perforated patch array, the interlaced elements array and some other configuration arrays derived from them. The review and comparison among them are presented in the following sections. Some advanced techniques to enhance DBDP antenna performances also are introduced.

2. DBDP perforated patch arrays

The DBDP antennas for SAR application are usually operating on two widely separated bands, causing great difference in dimensions of the radiators for dual bands. In order to keep the higher frequency (HF) radiator within a wavelength to suppress the grating lobes, the lower frequency (LF) radiators are perforated and the HF radiators are placed in the perforations. This type of array configuration is usually adopted when the frequency ratio of HF to LF is even. The example is an L/C-band perforated patch array by Shafai et al. (see

Fig. 2 and Fig.3) [12], where a perforated L-band patch and 16 C-bands patches form a unit cell with the frequency ratio of 4 : 1. The patches co-planarly configured in two bands are stacked to broaden the bandwidth, achieving a bandwidth for RL (return loss) ≤ -14 dB of 300 MHz at C-band (about 5.7%) and 90 MHz at L-band (about 6.4%). The patches of two bands are orthogonally fed to realize dual-polarization operation. The cross-polarization level in the bandwidth is lower than -30 dB. As seen from Fig.4, two slots of the C-band element are passive, but help in reducing the cross polarization to below -30 dB.

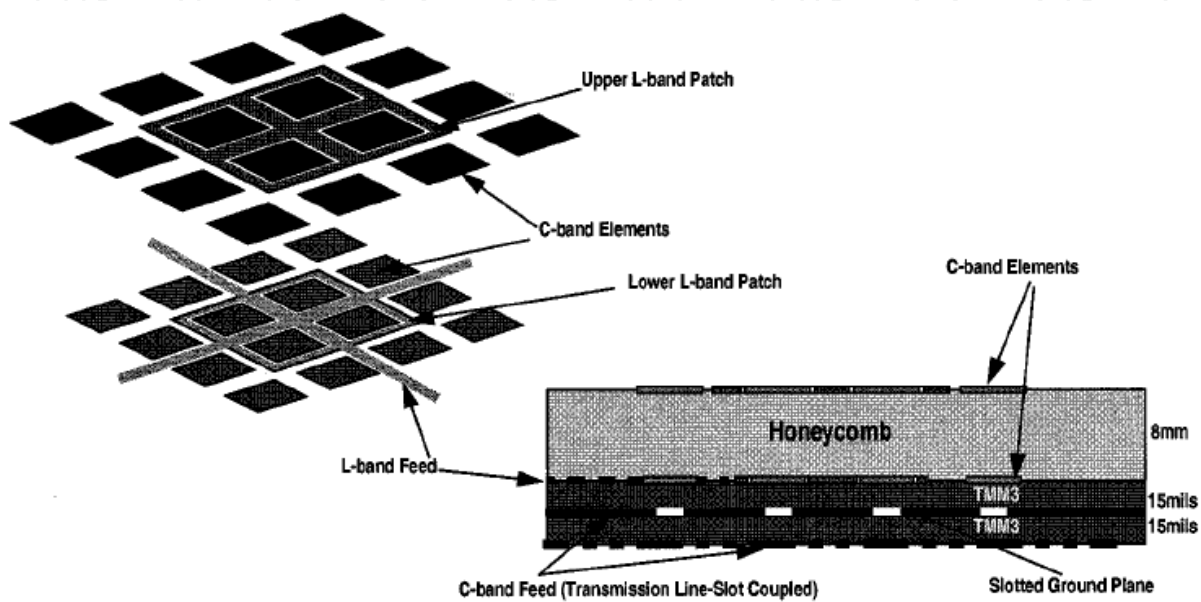


Fig. 2. L/C band perforated patch array[12]

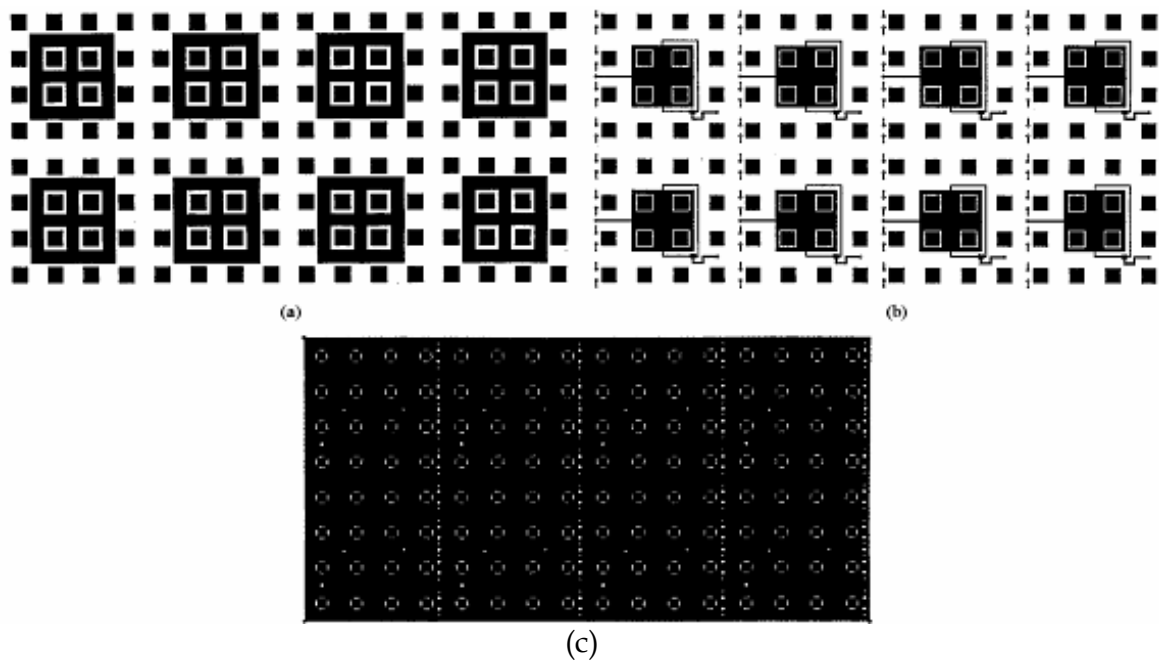


Fig. 3. Geometry of 2 x 4 unit-cell L-band subarray with C-band elements[12]
(a) Upper layer metallization showing passive patches (b) Lower layer metallization showing L-band feed (c)Ground plane metallization showing feed slots for C-band elements

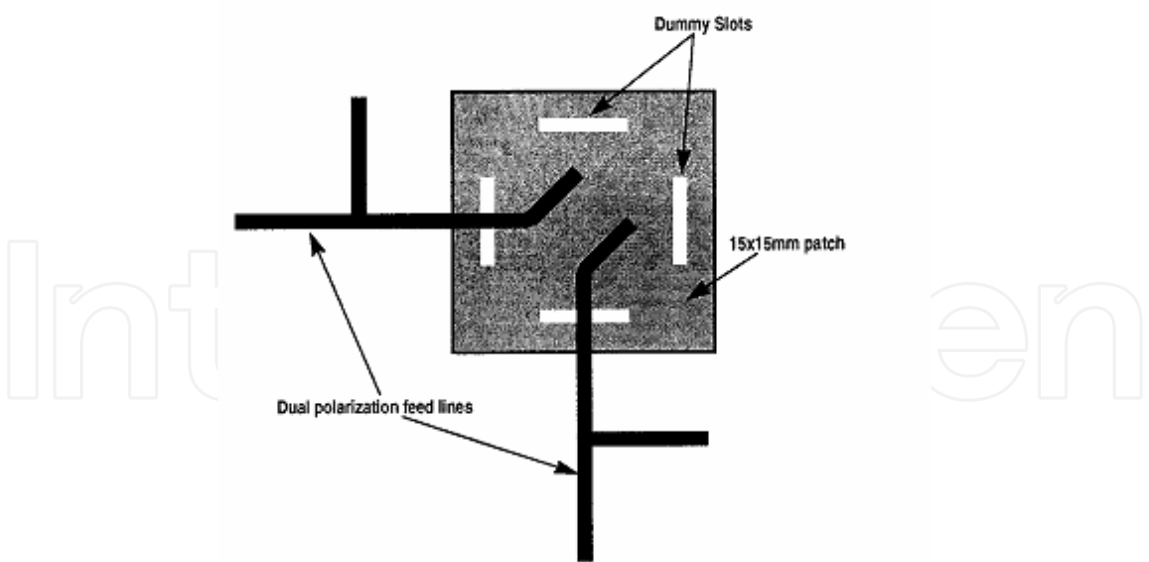


Fig. 4. Geometry of dual-polarized C-band element[12]

Another L/X DBDP array designed by Pozar and Targonski [13] uses the similar array configuration as shown in Fig. 5. The main advantage of this configuration is its wider bandwidth at LF compared with the other array designs, such as that of dipole/patch. But this will cause the difficulty in designing the antenna due to the dimension of perforation, which should be large enough to avoid hindering the radiation from HF elements. A larger

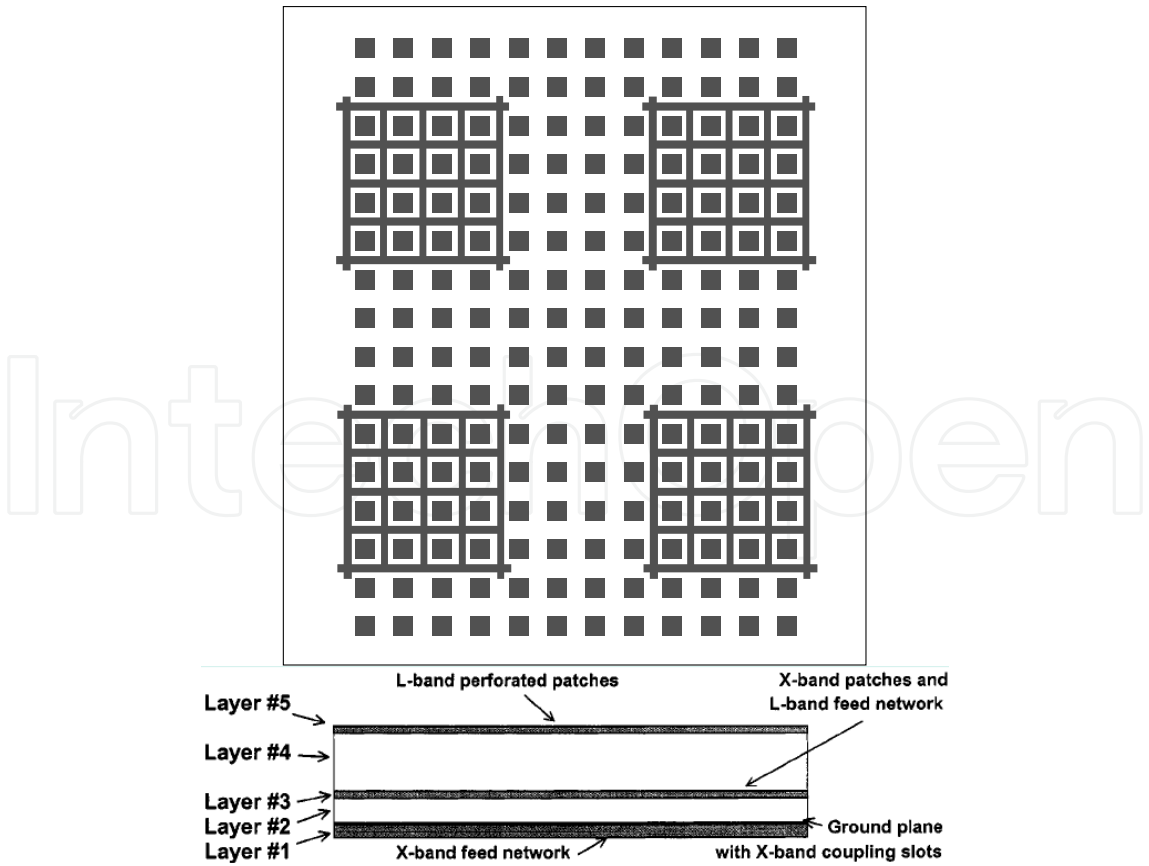


Fig. 5. Top view and side view of L/X-band DBDP antenna [13]

perforation size is also favored in terms of good isolation performance between the two bands and a more symmetric pattern at the cost of bandwidth at LF. Then a tradeoff must be made between the bandwidth and the isolation performance.

Recently a new element design of the DBDP perforated patch array has been reported, as shown in Fig.6 [14]. Its L-band antenna element is designed as a stacked perforated patches to ensure the required bandwidth(about 8%) and to allow for achieving integration with four C-band antenna elements. The perforated driven patch is excited by four probes, two of them generating vertical polarization and two generating horizontal polarization ,as shown in Fig 6b. Anti-phase excitations of the appropriate probes have been achieved with the use of 180° phase shifters realized as sections of transmission lines. Good return losses better than 15 dB and high isolation better than 30 dB have been achieved within the required broad frequency range. Two stacked square patches operating at C-band are fed through two orthogonally placed H-shaped slots as seen in Fig. 6c. Due to the limited space the feeding network of the vertical polarization is etched on the lower layer than that of the horizontal polarization. Good return losses better than 15 dB and high isolation better than 40 dB have been measured over the desired bandwidth (about 7 %) for a single C-band antenna element. The obtained cross-polarization level equals -20 dB.

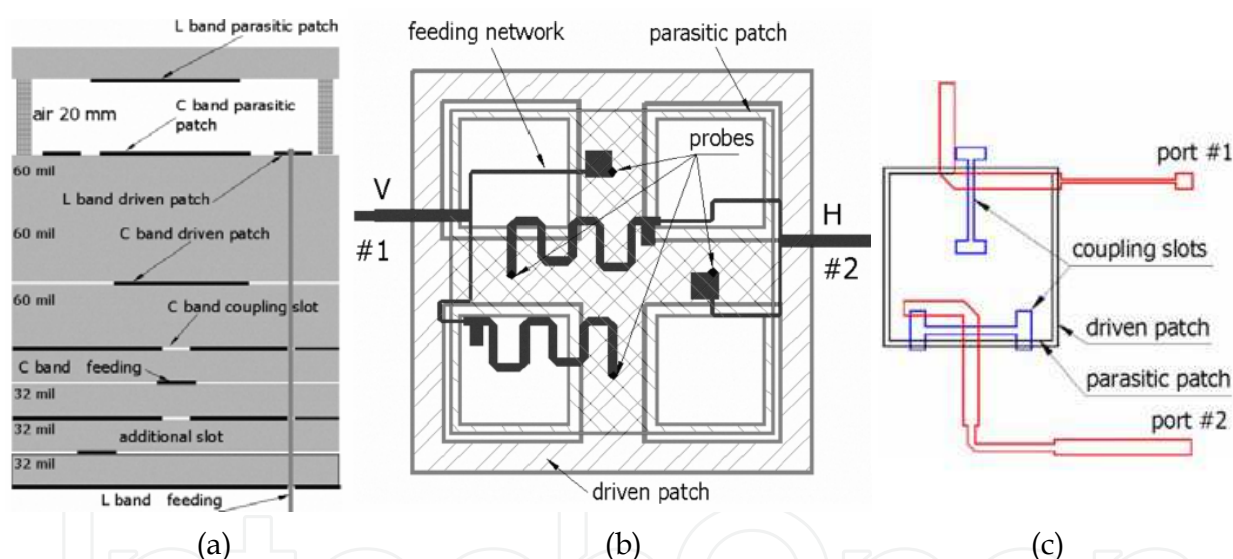


Fig. 6. L/C-band DBDP antenna element with the use of 180° phase shifters [14] (a) Cross-sectional view (b) Layout of L-band antenna element (c) Layout of C-band antenna element

3. DBDP interlaced elements arrays

3.1 Interlaced slot/dipole with patches

The DBDP array configuration of interlaced elements is attractive, where the element may be slot/dipole/ring or patch. Though an interlaced elements array employing either slots or printed dipoles for both bands and the architecture using microstrip patches for both bands may be considered [15], the shared-aperture DFDP array of interlaced slot/dipole with patches is often preferred. Because of its smaller size in one dimension, the slot/dipole of LF can be easily placed between two HF elements, thus meeting the interelement-distance requirement. An example is the DBDP L/C band array of the interlaced L-band slots with C-

band patches designed by Pozar et al. (see Fig. 7) [16], where C-band square patches are located on the top layer and L-band slots on the ground. The slots are orthogonally placed to realize the dual-polarization in L-band. This design achieves a bandwidth more than 5% in both bands and the isolation is better than 24 dB in C-band and 23 dB in L-band. But to suppress the backward radiation of the slots, a reflector is placed $1/4$ wavelength behind the slot and therefore the dimension of the array is increased.

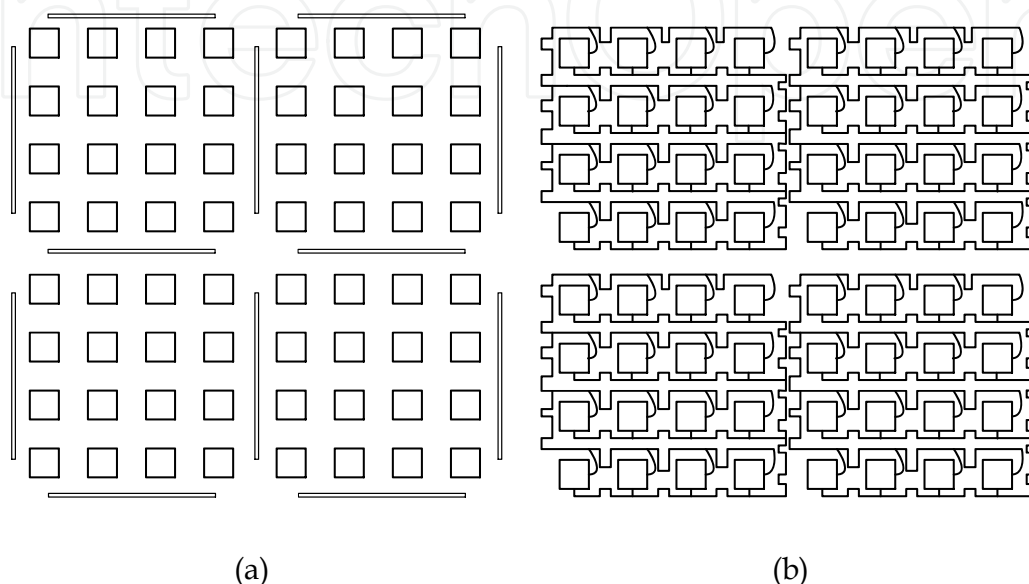


Fig. 7. L/C band Interlaced slots with patches[16] (a) Top layer parasitic patch; (b) driven patch with feed

In another example, S/X band interlaced dipoles with patches are proposed by our group [7,8] as shown in Fig. 8, where both stacked patches and stacked dipoles are adopted, which achieves a measured bandwidth of 8.9% and 17% in S-band and X-band, respectively, with its frequency ratio of about 1 : 3, as shown in Fig. 9. Since the S-band dipoles are cross-placed and located on another side of the substrate, the cross-polarization and the isolation between two ports at S-band are minimized, resulting in the cross-polarization levels of better than -26 dB and -31 dB at S-band and X-band, respectively. In addition, by using dipoles instead of slots, the serious backward radiation is avoided. However, the bandwidth of dipole is usually narrower than that of slot, so a stacked dipole is used and another substrate is needed compared to the interlaced slot/patches array aforementioned. From the radiation patterns of both bands depicted in Fig.10, it is obvious that the arrays of both bands have little impact on each other radiation patterns--from the shape and null points of patterns, so they look like working "separately".

Recently, a similar configuration [17] is reported to apply to the millimeter wave band as a feed of a parabolic cylindrical reflector antenna. The Ka-band microstrip patches working at 35.5GHz are in the upper layer and interlaced with the Ku-band cross slots working at 13.6 GHz. Dual-polarizations have realized for the Ku-band, but only single-polarization has realized for the-Ka band since space constraint. By sharing the same antenna aperture, the problem of placing two feeds at one focus is solved.

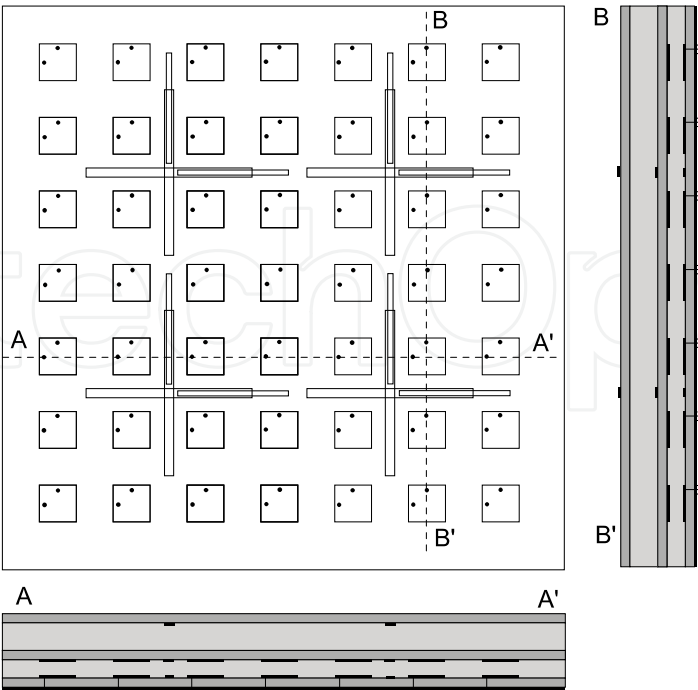


Fig. 8. S/X-band interlaced dipole with patches

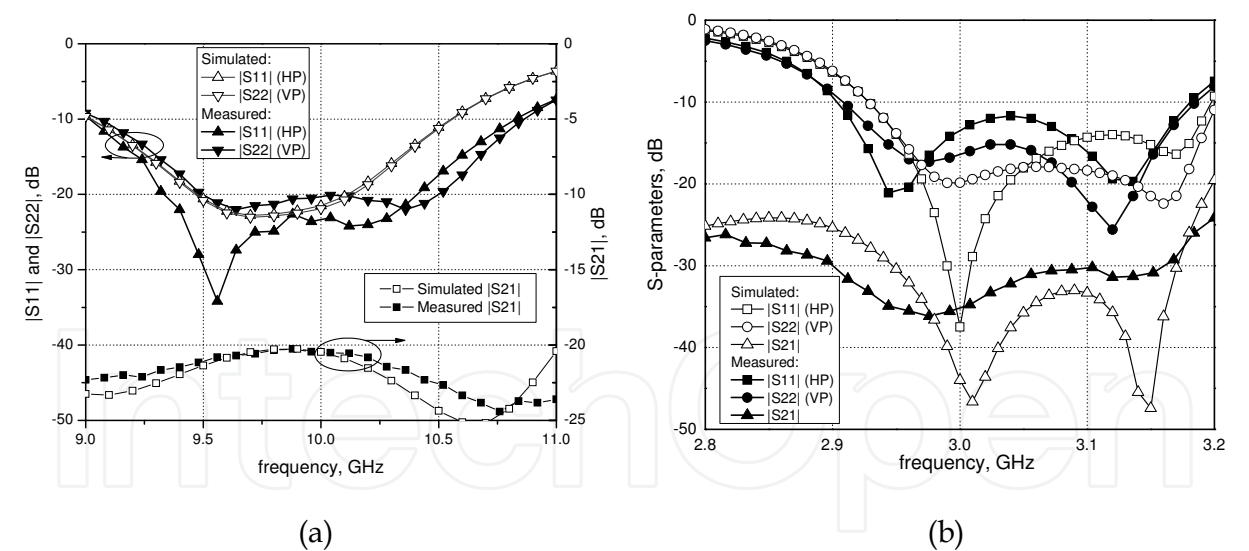


Fig. 9. Measured *S* parameter of S/X-band array. (a) X-band element; (b) S-band element

The feed array consists of 8 Ku-band elements linear arrays and 16 Ka-band elements linear arrays, and top view of the half-model (4 Ku- and 8 Ka-band elements linear arrays) is shown in Fig.11a, where a Ku-band linear array includes 2 cross slots and a Ka-band one includes 4 microstrip patches. Fig.11b shows the cross-sectional view. Since the slot is bidirectional, 4 mm-thick reflector ground plane is used at a distance of about $\lambda/4$ behind the cross slot. This design has achieved satisfactory performances in both bands, verifying the validity for the millimeter wave band application.

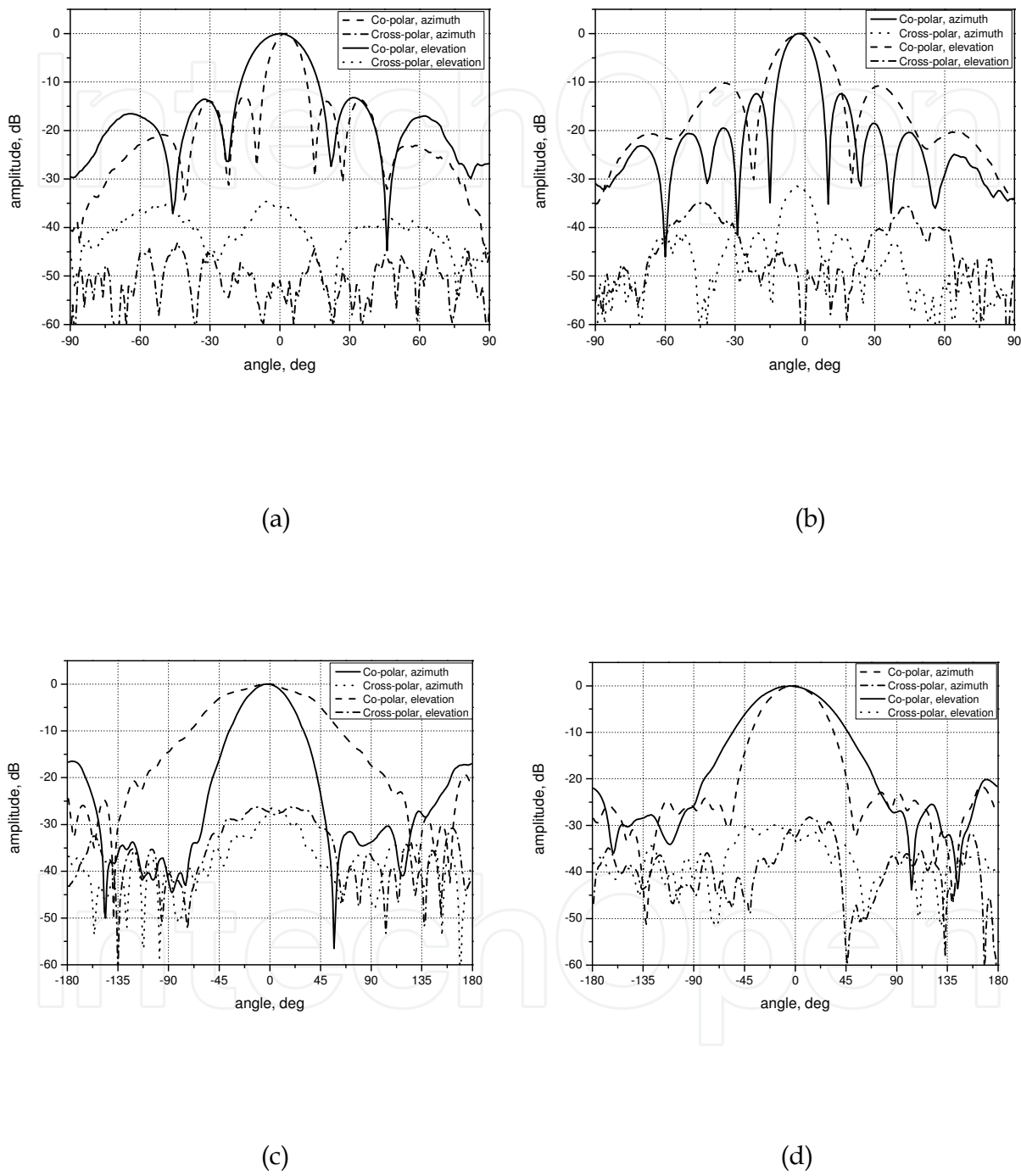


Fig. 10. Measured radiation pattern of S/X-band array. (a) H-polarization of X-band; (b) V-polarization of X-band; (c) H-polarization of S-band; (d) V-polarization of S-band

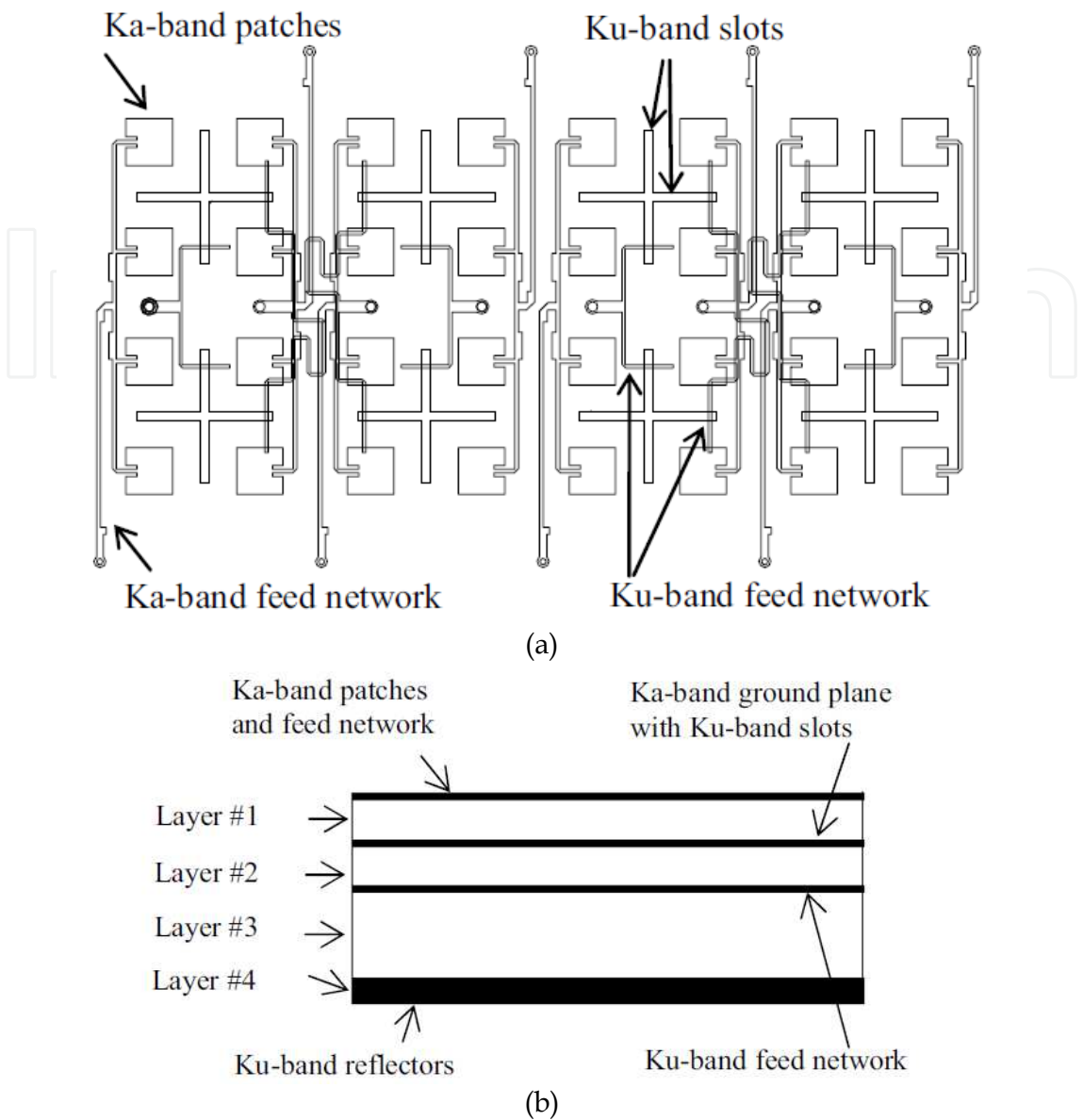


Fig. 11. Ka/Ku array of interlaced cross-slots with patches [17] (a) Top view (b) cross-sectional view

3.2 Interlaced ring with patches

A DBDP array consisting of interlaced ring with patches for airborne applications is presented in [18]. The S-band antenna elements sit on the top layer, and the X-band antennas are on the bottom layer. These two planar arrays with thin substrates are integrated to provide simultaneous operation at S-band (3 GHz) and X-band (10 GHz), as shown in Fig.12a. The X-band antenna elements are circular patches. They are combined to form a 4×8 array with a gain of 18.3 dBi, using the 4 element series-fed resonant type arrays to save the space of the feeding line network, as shown in Fig. 12b. The S-band element is a large rectangular ring-resonator antenna. The four sides of the square-ring element are laid out in such a way that they only cover part of the feeding lines on the bottom layer, but none of the radiating elements. The antenna has a mean circumference of about $2\lambda_g$ and has a 9.5 dBi gain that is about 3 dB higher than the gain of an ordinary ring antenna. The ring is

loaded by two gaps of its parallel sides, and these make it possible to achieve a 50Ω input match at the edge of the third side.

Measured normalized radiation patterns for both bands are shown in Fig.13 and Fig.14. The measured and simulated specifications of the S/X-band array are summarized in Table 2. It is seen that its performances are quite good, but the bandwidths are narrow due to its thin structure, while the thin and lightweight structure is attractive for airborne applications.

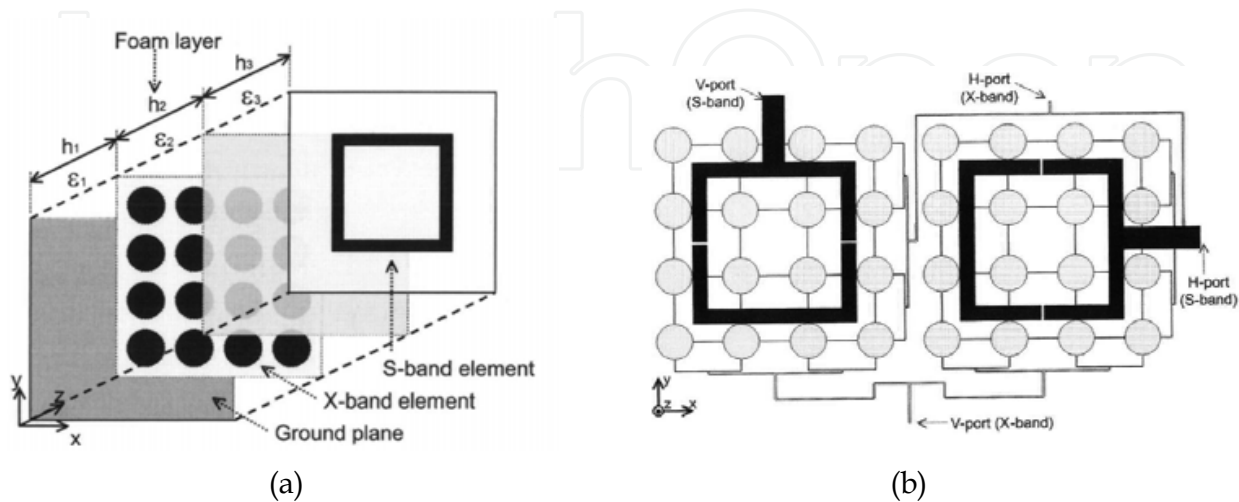


Fig. 12. S/X-band array of interlaced rings with patches[18]
(a) multilayer structure (b) Top view

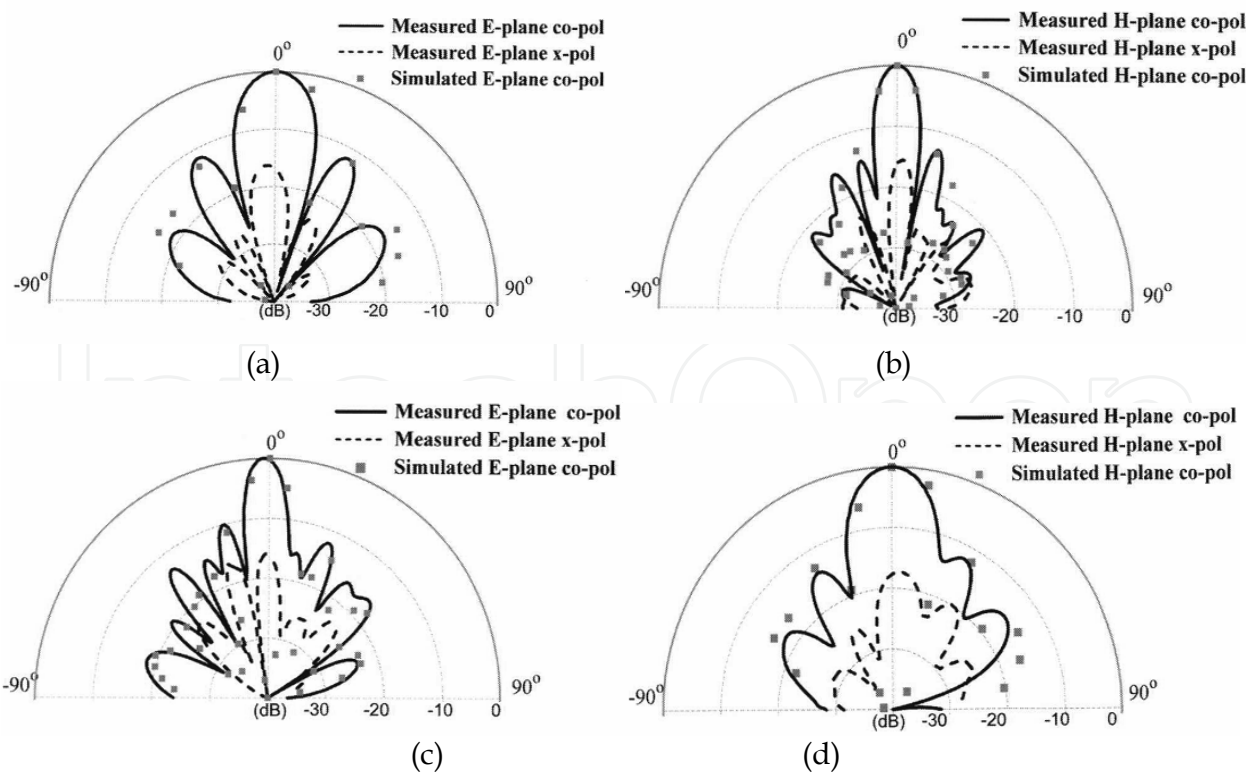


Fig. 13. Radiation patterns of the X-band array[18]
(a) V-port feed, E-plane (b) V-port feed, H-plane
(c) H-port feed, E-plane (d) H-port feed, H-plane

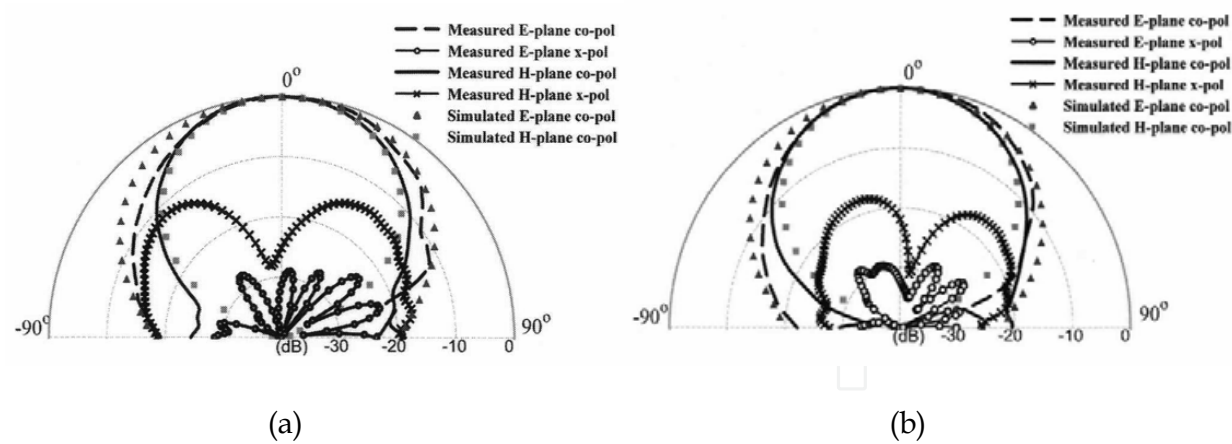


Fig. 14. Radiation patterns of the S-band array[18] (a)V-port feed (b) H-port feed

		X-Band		S-Band	
	Polarization	V Port	H Port	V Port	H Port
Frequency (GHz)	Measurement	9.8-9.98	9.81-10.0	2.94-2.96	2.94-2.96
	Simulation	9.91-9.99	9.9-10.0	2.94-2.96	2.94-2.96
Bandwidth (%)	Measurement	1.8	2.3	1.03	1.03
	Simulation	1.0	1.0	1.03	1.03
Gain (dBi)	Measurement	18.3	17.3	9.5	7.9
	Simulation	17.6	17.6	8.72	8.73
Efficiency (%)	Measurement	32.4	28.8	96.8	66.8
	Simulation	27.5	27.5	80.9	80.9
HPBW (degrees)	E plane	17°	8.9°	58°	59°
	H plane	9.5°	17.4°	53°	52°
Peak SLL (dB)	Measurement	-12.3	-10.0	None	None
	Simulation	-13.0	-13.0		
FBR (dB)		-30	-30	-34.8	-25.5
Isolation (dB)		> 31.1	> 25.3	> 36.4	> 33.8
		X to S band	X to S band	S to X band	S to X band

Table 2. A summary of the measured and simulated results for the S/X -band array[18]

3.3 Interlaced cross-patch with patches

An S/X-band cross-patch/patch array is proposed by Salvador *et al* in Ref. [19] (See Fig. 15). Its S-band cross-patch and X-band patches are co-planarly interlaced. It may be seen as the corner-removed perforated patch (L-band perforated patch in Fig. 2) or the co-plane cross-placed dipole (S-band dipole in Fig. 8). The bandwidth of the cross-patch is proportional to the width of its “leg”, which is constrained by the inter-element distance. An obvious drawback is that if the gap between two bands is narrow (the leg of cross-patch is too wider), serious inter-band couple may be caused and the radiation pattern will be distorted.

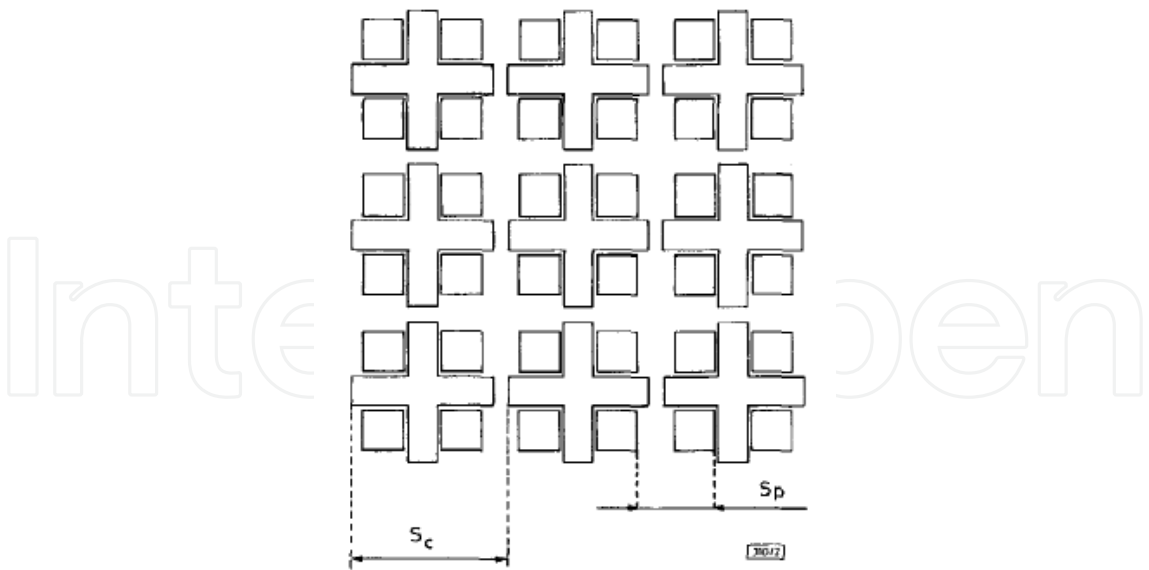


Fig. 15. S/X-band array of interlaced cross-patches with square patches [19]

4. DBDP other configuration arrays

Some other array configurations have also been proposed, most of which can be classified as the deriving forms of the two basic types mentioned in Sects. 2 and 3. One example is the L/C-band array of interlaced L-band perforated cross-patches with C-band patches, whose top view and cross section are shown in Fig. 16[10]. The LF perforated cross-patch on the top layer is interlaced and rounded by 9 HF patches located on another substrate behind it to form a unit cell. The unit cells are cascaded-fed to make up a traveling wave linear sub-array [11], and then a linear sub-array is used to construct a sub-array. Benefiting from its “H”-shape slot aperture coupled in both bands, the simulated cross-polarization at dual bands are claimed to be less than -40 dB, and the backward radiation is also small enough. However, the isolation performance may probably be a problem.

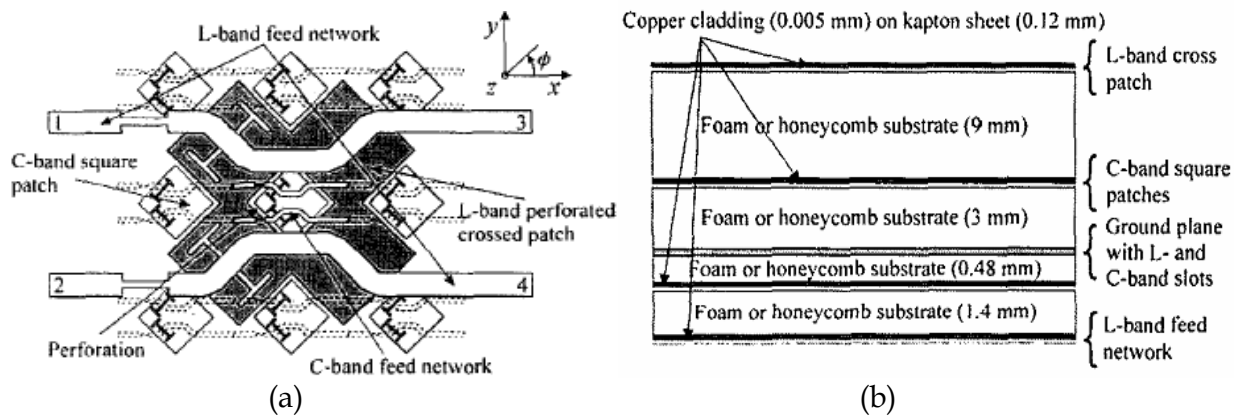


Fig. 16. L/C-band perforated cross-patch/patches array[10] (a) top view (b) cross-sectional view

As an additional example, a DBDCP(dual-band dual-circular-polarization) element is shown in Fig.17[20] [21]. A square shorted-annular-ring element operates at a low frequency band,

and using notches at two opposing corners of the element’s outer ring produces a circular polarization with a single-point feeding. Shorting the inner square ring of the shorted-annular-ring element creates an area that can be used for a printed square slot that operates at a higher frequency band. The slot element can be perturbed by notching two opposite corners to produce a circular polarization. The printed slot can be fed with a stripline that runs under the annular ring structure.

An element was designed with the goal to cover the 2.45 GHz and 5.8 GHz ISM (Industrial, Scientific and Medical) bands with dual-CP operation at each band [21]. The simulated S-parameters show that the isolation between the high and low band ports is better than 25dB. The isolation between the two high band ports has a maximum value greater than 40dB at the center of the band, while that between the low band ports is lower than the former.

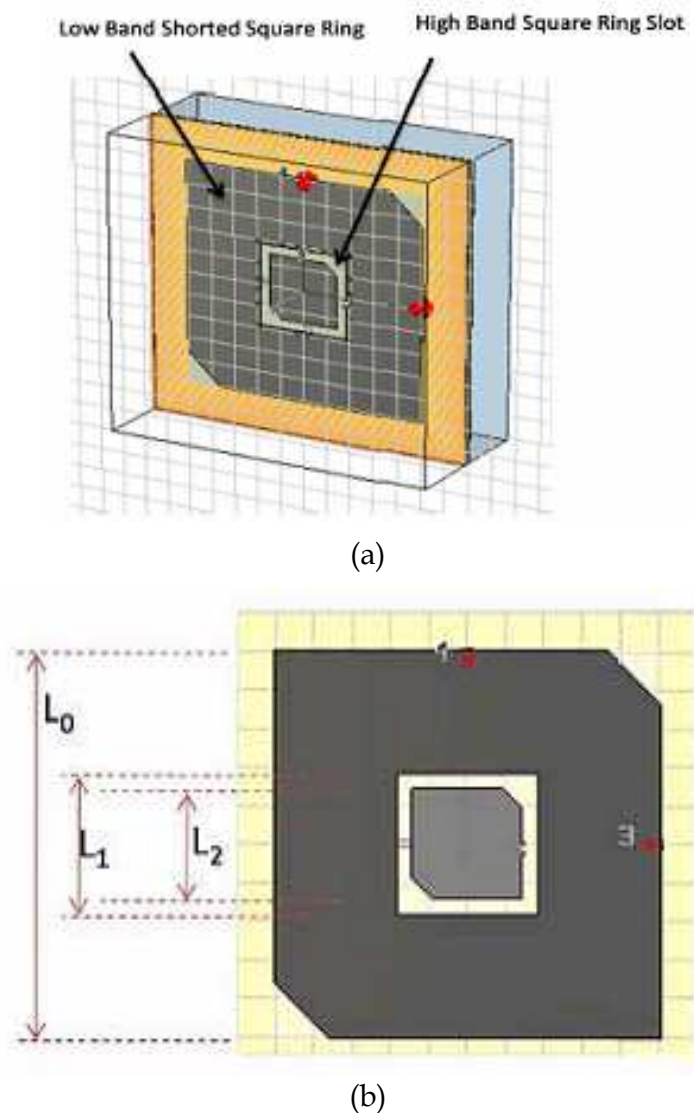


Fig. 17. Geometry of the dual-band, dual- CP element [21] (a) Isometric view (b) Top view

5. Comparison of DBDP arrays

A comparison of several DBDP designs is listed in Table 2, where some measured results of a new design with the “interlaced dipole and patch” configuration [22] is also included.

Generally evaluating from the listed three performances, it is seen that the “interlaced dipole and patch” configuration may be one of the best choices. In general, the arrays of interlaced slots/dipoles/rings with patches are preferred. Moreover, their flexibility in array configuration makes them more attractive.

array configuration	bandwidth	cross-polarization	port isolation	cross-band isolation
perforated patch [12] (in Fig. 2)	L: 6.4% C: 5.7%	L: about -32 dB (peak) C: ≤-30 dB	— —	— —
perforated patch [13] (in Fig. 5)	L: ≥6% X: ≥10%	L: about -22 dB (peak) X: ≤-20 dB	L: ≤-20 dB X: ≤-18 dB	≤-40 dB in both bands at both polarization
interlaced slot and patch [16] (in Fig. 7)	L: ≥5% C: ≥5%	L: ≤-23 dB C: ≤-24 dB	— —	L: ≤-15 dB C: ≤-40 dB
interlaced dipole and patch [7] (in Fig. 8)	S: ≥8.9% X: ≥17%	S: ≤-26 dB X: ≤-31 dB	S: ≤-20 dB X: ≤-20 dB	— —
interlaced dipole and patch[22]	S: ≥11.4% X: ≥13.9%	— —	S: ≤-35 dB X: ≤-25 dB	— —
interlaced slot and slot [15]	C:5% X: 2%-3% (VSWR≤1.5)	C: ≤-21 dB X: ≤-18 dB	— —	— —

Table 2. Comparison of various DBDP designs

6. Techniques of enhancing DBDP antenna performances

6.1 Pair-wise anti-phase feeding technique

The cross-polarization level of a DBDP antenna is influenced by the figure of its element, the feeding form and the array configuration. In general, more symmetric element shape and thinner substrate (for the patch element) will lead to a lower cross-polarization level. Besides these, the “pair-wise anti-phase feeding technique” is proposed (see Fig. 18) [23, 24]. The neighboring patches are mirror configured and anti-phase fed in H-port or in V-port, and thus all elements in subarray are of same effective excitation and the cross-polarization level is obviously improved at the boresight. As to the cost, in the area out of main beam, the cross-polarization level is raised.

6.2 Symmetrical feeding technology

As introduced in 6.1, the cross-polarization level can be improved by the “pair-wise anti-phase feeding technique” in array, while the port isolation of array is just about completely decided by element port isolation itself. Therefore, the main task in element designing is to achieve good port isolation and after that is the low cross-polarization characteristic. Since a circular patch generally works at TM₁₁ mode, its current components orthogonal to the primary components will result in worse cross-polarization characteristic. Thus, the square patch is preferred. For its dual-polarized operation, a symmetrical feeding technology [25]

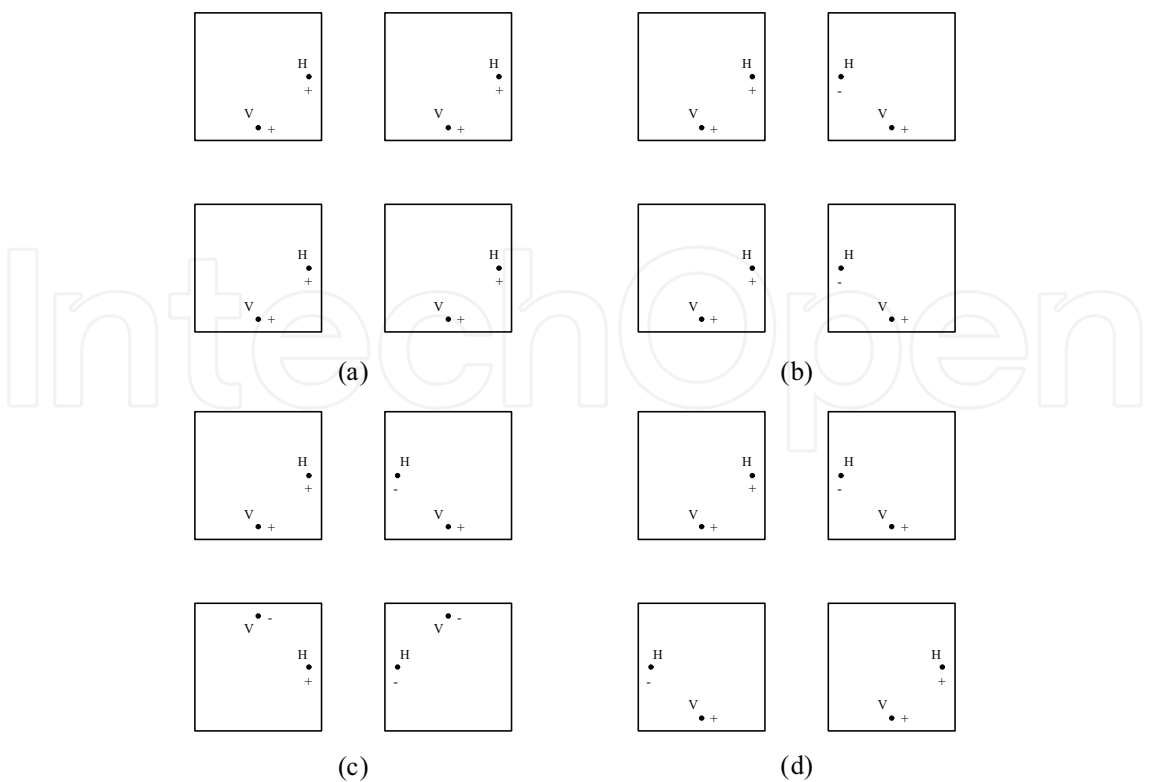


Fig. 18. Subarray configuration [23] (a) distant HH– (b) close HH– (c) HH– & VV– (d) distant & close HH–

is shown in Fig.19, where the stacked parasitic patch has been used to broaden the bandwidth. From the view of symmetry, an aperture-coupled feed located at the center of patch is chosen firstly. In order to increase the coupling between feed line and patch, the “H”-shaped slot is adopted. The simulated results in [25] show that the cross-polarization level of the patch with a pair of edge feeds is -36dB and that with a center feed is -42dB, about 6dB better than the former. Another merit of the center feed is that the slot at center can give a good coupling level and the front-back ratio of patch is improved. As for the another polarization, the balanced edge feeding is adopted to keep the symmetry. Two balanced pin-feeds are connected by the feed network which is carefully tuned to realize accurate “equal and anti-phase feed”. Then a microstrip line is used to realize impedance matching.

Fig.20 is the simulated S parameters for two ports. It is seen that the balanced pin-feed port achieves an impedance bandwidth (Return loss \leq -10dB) of 840MHz (5.01GHz-5.85GHz) and the aperture couple port of 850MHz (5.09GHz -5.94GHz), while the port isolation keeps under -43dB .The simulated cross-polarization within the main lobe remains less than -37dB in whole bandwidth. The calculated gain of antenna is stable at the 9dB while the front-back ratio keeps better than 22dB in the whole bandwidth.

6.3 Slot-loaded patch for improving port isolation

It is proposed to etch a slot in the corner of a driven patch by our group [26] (see Fig. 21). The effect of using the slot-loaded method can be seen from Fig. 22, where the isolation level between two ports is improved for at least 5 dB. However, the field under the patch is

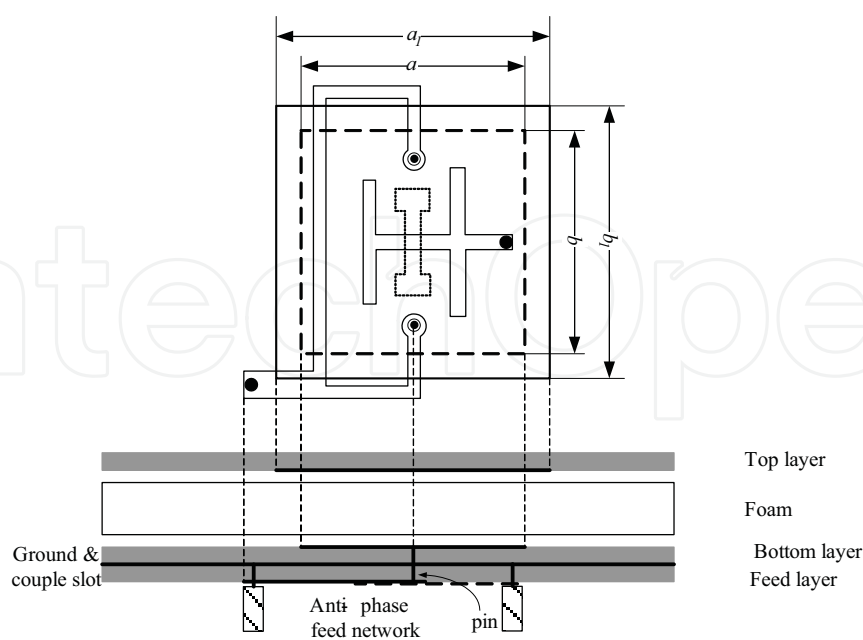


Fig. 19. Configuration of antenna element

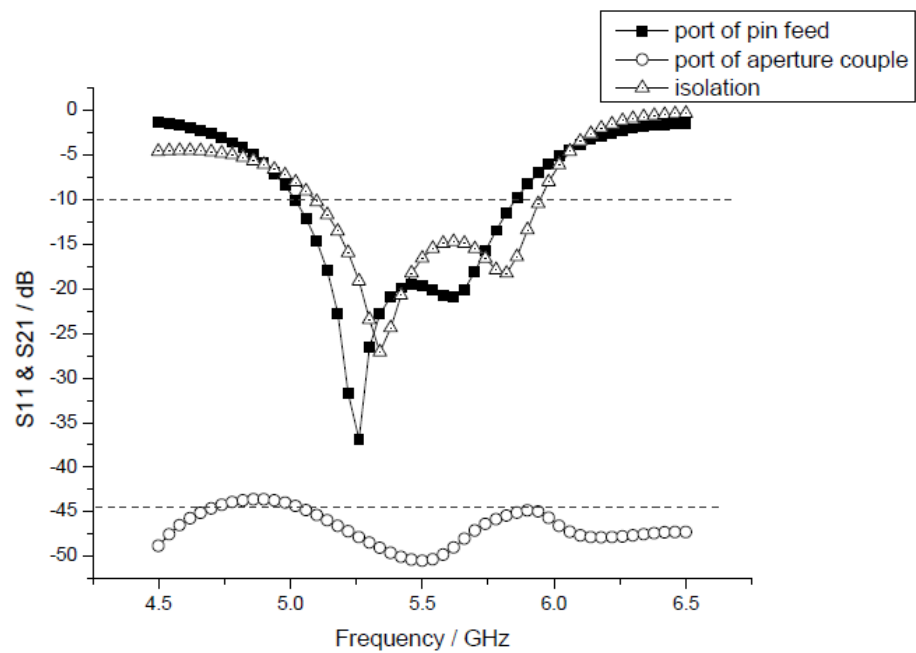


Fig. 20. S parameters of antenna element

disturbed by the slot, then the cross-polarized field is brought out and the cross-polarization level deteriorates. In Ref. [27], a similar method is adopted. The only difference is that “T”-shaped slot and some edge-slot are etched on the driven patch, which also achieves a good isolation.

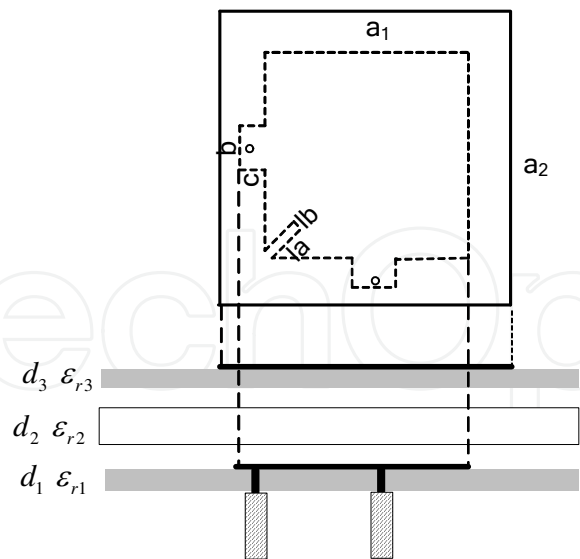


Fig. 21. Slot-loaded patch

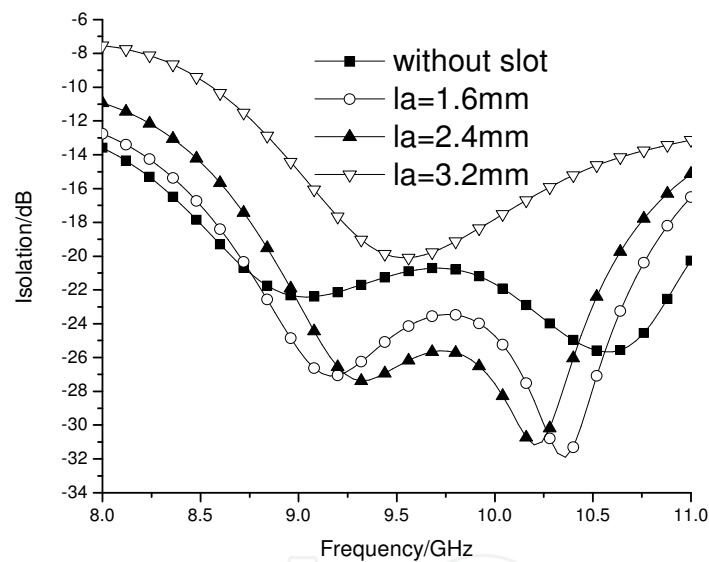


Fig. 22. Isolation S_{12} for various slot lengths

6.4 Bandwidth enhancement technique

The SAR systems use the impulse compression technology to realize the high-resolution at elevation direction and thus a wider bandwidth is required for the antenna to radiate narrower impulse (in time domain). An antenna system can not broaden bandwidth by means of array synthesis, and the antenna bandwidth generally lies on its element bandwidth. Therefore, a lot of bandwidth enhancement methods for antenna elements have been proposed, such as co-planar/stacked parasitic patches. In DBDP antenna array design, the distance between elements is limited by the scanning requirement and the using of stacked parasitic patches is probably the most effective broadening method for its room saving structure, which can achieve at least a bandwidth of 15% [26], about three times of that of a conventional patch.

7. Conclusion

The dual-band dual-polarization (DBDP) shared-aperture microstrip array technology for the synthetic aperture radar (SAR) application in the last decade has been reviewed. Several designs of DBDP SAR antenna arrays are introduced with their main performances, then their comparison is summarized. According to the configuration, the basic DBDP arrays include two types: the perforated patch array and the interlaced elements array. In the general, the arrays of interlaced slots/dipoles/rings with patches are preferred. Moreover, their flexibility in array configuration makes them more attractive. In addition, tri(or more)-band dual-polarization shared-aperture microstrip arrays for the SAR applications may be formed by means of different DBDP arrays[28]. Finally, some techniques enhancing DBDP antenna performances also have been presented.

8. Acknowledgements

This work was supported by the National Natural Science Foundation of China (Grant No. 60871030), and the National High-Technology Research and Development (863) Project of China (Grant No. 2007AA12Z125).

9. References

- [1] Zhang Z Z. Guide of Airborne and Spaceborne SAR system. Publish House of Electronics Industry, Beijing, 2004 (in Chinese)
- [2] Zhong S S, Cui J H. A new dual-polarized aperture-coupled printed array for SAR application. *Journal of Shanghai University (English Edition)*, 2001, 5(4): 295-298
- [3] Du X H, Li J X, Zheng X Y. Design of X-band dual-polarized active phased array. *Modern Radar*, 2002, 18(5): 67-70 (in Chinese)
- [4] Zhong S S, Yang X X, Gao S C, Cui J H. Corner-fed microstrip antenna element and arrays for dual-polarization operation. *IEEE Transactions on Antennas and Propagation*, 2002, 50(10): 1473-1480
- [5] Wang W, Zhong S S, Liang X L. A dual-polarized stacked microstrip antenna subarray for X-band SAR application. *IEEE Antennas and Propagation Society International Symposium*, Monterey, CA, 2004: 1603-1606
- [6] Wang W, Li L, Zhang Z H. Dual-polarized space-borne SAR antenna array. *Remote Sensing Technology and Application*, 2007, 22(2): 166-172 (in Chinese)
- [7] Qu X, Zhong S, Zhang Y, and Wang W. Design of an S/X dual-band dual-polarised microstrip antenna array for SAR applications. *IET Microwave, Antennas, and Propagation*, 2007, 1(2): 513-517
- [8] Zhong S S, Qu X, Zhang Y M, and Liang X L. Shared-aperture S/X dual-band dual-polarized microstrip antenna array. *Chinese Journal of Radio Science*, 2008, 23(2): 305-309
- [9] Zhai G H, Hu M C, Li J X. A novel dual-polarization microstrip patch antenna for space-borne SAR application. *Modern Radar*, 2007, 29(4): 72-75 (in Chinese)

- [10] Vallecchi A, Gentili G B, Calamia M. Dual-band dual polarization microstrip antenna, IEEE Antennas and Propagation Society International Symposium, Columbus, OH, 2003: 134-137
- [11] Granet C, Zhang H Z, Greene K J, James G L, Forsyth A R, Bird T S, Manchester R N, Sinclair M W, Sykes P. A dual-band feed system for the Parkes radio telescope, IEEE Antennas and Propagation Society International Symposium , Boston., MA, 2001: 296-299
- [12] Shafai L L, Chamma W A, Barakat M, Strickland P C, Seguin, G. Dual-band dual-polarized perforated microstrip antennas for SAR applications. IEEE Transactions on Antennas and Propagation, 2000, 48(1): 58-66
- [13] Pozar D M, Targonski S D. A shared-aperture dual-band dual-polarized microstrip array. IEEE Transactions on Antennas and Propagation, 2001, 49(2): 150-157
- [14] Wincza K, Gruszczynski S, Grzegorz J ,Integrated dual-band dual-polarized antenna element for SAR applications, IEEE 10th Annual Wireless and Microwave Technology Conference (WAMICON'09), Clearwater, FL, 2009: 1 - 5
- [15] Pokuls R, Uher J, Pozar D M. Dual-frequency and dual-polarization microstrip antennas for SAR applications. IEEE Transactions on Antennas and Propagation, 1998, 46(9): 1289-1296
- [16] Pozar D M, Schaubert D H, Targonski S D, Zawadski M. A dual-band dual-polarized array for spaceborne SAR. IEEE Antennas and Propagation Society International Symposium, Atlanta. GA, 1998: 2112-2115
- [17] Gao G.M., Y.M. Zhang Y.M., Li Ang, Zhao J.M., Cheng H. Shared-aperture Ku/Ka bands microstrip array feeds for parabolic cylindrical reflector, 2010 International Conference on Microwave and Millimeter Wave Technology (ICMMT2010), Chengdu, China, 2010 : 1028-1030
- [18] Hsu S.H., Ren Y.J., and Chang K. A dual-polarized planar-array antenna for S-band and X-band airborne applications, IEEE Antennas and Propagation Magazine, 2009 , 51(4):70-77
- [19] Salvador C, Borselli L, Falciani A, Maci S. Dual frequency planar antenna at S and X bands. Electronics Letters, 1995, 31(20): 1706-1707
- [20] Zaghloul A. I. and Dorsey W. M. Evolutionary Development of a Dual-Band, Dual-Polarization, Low-Profile Printed Circuit Antenna, International Conference on Electromagnetic in Advanced Application, Torino, Italy, 2009: 994-997
- [21] Dorsey W.M. and Zaghloul A.I. Dual-polarized dual-band antenna element for ISM bands, IEEE International Symposium on Antennas and Propagation, Charleston, South Carolina, 2009:1-4
- [22] Zhong S-S, Sun Z. S/X dual-band dual-polarization microstrip dipole/stacked patch array antenna, Invention Patent of China (Applied), No.201010275934.8, Date:08-09-2010 (in Chinese)
- [23] Woelders K, Granholm J. Cross-polarization and sidelobe suppression in dual linear polarization antenna arrays, IEEE Transactions on Antennas and Propagation, 1997, 45(12): 1727-1740

- [24] Liang X-L, Zhong S-S , Wang W. Cross-polarization suppression of dual-polarization microstrip antenna arrays, *Microwave and optical technology Letters*, 2004, 42(6): 448-451
- [25] Sun Z, Zhong S-S, Tang X-R, Liu J-J. C-Band Dual-Polarized Stacked-Patch Antenna with Low Cross-Polarization and High Isolation, 3rd European Conference on Antennas and Propagation(EuCAP2009), Berlin, Germany, 2009:2994-2997
- [26] Chen K D, Zhong S-S, Yan X-R. Design of S/X dual-band dual-polarized shared-aperture microstrip antenna array. *Journal of Microwaves*, 2008, 24(6):65-67 (in Chinese)
- [27] Zaman A U. Dual polarized microstrip patch antenna with high port isolation. *Electronics Letters*, 2007, 43(10): 551-552
- [28] Zhong S-S, Sun Z and Kong L-B. L/S/X tri-band dual-polarization planar array antenna, Invention Patent of China (Applied), No.201010275940.3, Date:08-09-2010 (in Chinese)

IntechOpen



Microstrip Antennas

Edited by Prof. Nasimuddin Nasimuddin

ISBN 978-953-307-247-0

Hard cover, 540 pages

Publisher InTech

Published online 04, April, 2011

Published in print edition April, 2011

In the last 40 years, the microstrip antenna has been developed for many communication systems such as radars, sensors, wireless, satellite, broadcasting, ultra-wideband, radio frequency identifications (RFIDs), reader devices etc. The progress in modern wireless communication systems has dramatically increased the demand for microstrip antennas. In this book some recent advances in microstrip antennas are presented.

How to reference

In order to correctly reference this scholarly work, feel free to copy and paste the following:

Shun-Shi Zhong (2011). DBDP SAR Microstrip Array Technology, Microstrip Antennas, Prof. Nasimuddin Nasimuddin (Ed.), ISBN: 978-953-307-247-0, InTech, Available from:

<http://www.intechopen.com/books/microstrip-antennas/dbdp-sar-microstrip-array-technology>

INTech
open science | open minds

InTech Europe

University Campus STeP Ri
Slavka Krautzeka 83/A
51000 Rijeka, Croatia
Phone: +385 (51) 770 447
Fax: +385 (51) 686 166
www.intechopen.com

InTech China

Unit 405, Office Block, Hotel Equatorial Shanghai
No.65, Yan An Road (West), Shanghai, 200040, China
中国上海市延安西路65号上海国际贵都大饭店办公楼405单元
Phone: +86-21-62489820
Fax: +86-21-62489821

© 2011 The Author(s). Licensee IntechOpen. This chapter is distributed under the terms of the [Creative Commons Attribution-NonCommercial-ShareAlike-3.0 License](https://creativecommons.org/licenses/by-nc-sa/3.0/), which permits use, distribution and reproduction for non-commercial purposes, provided the original is properly cited and derivative works building on this content are distributed under the same license.

IntechOpen

IntechOpen